

# Development of a predictive method to analyze the effect of “new” gases on soot formation based on Laser Induced Incandescence measurements

P. Visser\*, V.M. van Essen and H.B. Levinsky  
DNV GL Oil & Gas, P.O. Box 2029, 9704 CA Groningen, the Netherlands

## Abstract

We have developed a method for characterizing sooting tendencies for gases. Towards this end, soot volume fractions were measured using laser-induced incandescence (LII) in rich-premixed Bunsen-type flames with varying fuel compositions of  $C_2H_6$ ,  $C_3H_8$ ,  $C_4H_{10}$ ,  $N_2$ ,  $CO_2$  and  $H_2$  in  $CH_4$ . Upon the addition of higher hydrocarbons to methane the sooting tendency was observed to increase, while for the inert gases the sooting tendency decreased. A correlation was found between propane equivalent (PE) and the actual soot volume fractions for the binary hydrocarbon mixtures. The addition of hydrogen either increases or decreases the soot volume fraction depending on the fuel composition. This behavior for hydrogen is at present poorly understood. All measurements were used as input for an analysis to yield a regression equation for comparison of gases based on their sooting tendency at equivalence ratios where soot formation, deposition and emission may occur in end-use appliances. Comparison of the experimental results with predictions using the regression equation shows that the method can rank gases based on their sooting tendencies with reasonable accuracy.

## 1. Introduction

Diminishing local natural gas reserves, increasing geographical diversity of the gas supply and the desire to introduce sustainable fuels into the gas infrastructure are increasing the range of gas compositions being offered to the gas grid. These gases, which contain varying fractions of methane, higher hydrocarbons, carbon dioxide, nitrogen and in the near future perhaps hydrogen, may have different tendencies to soot than traditionally distributed gases. Possible soot formation due to new gases in end-use equipment may cause soot deposition, resulting in clogging and safety issues, while in equipment dependent on soot, soot formation may diminish.

An earlier method has been developed for characterizing soot tendencies using “yellow tipping” phenomena in domestic end user appliances with Bunsen type flames, such as gas cookers, instantaneous hot water heaters and conventional boilers [1]. This method is based on experiments performed in the 1950’s [2] and can be used to assess the first stages of soot formation indicated by yellow tipping, which is relevant for approval standards for some appliances in the European Union. For other types of equipment, such as instantaneous hot water heaters and central-heating boilers, approval standards allow yellow tipping but not soot deposition or emission. For gas fireplaces, some soot deposition and emission are allowed and soot formation is even a prerequisite for the proper functioning of the appliance. There is currently no method to predict the tendency for soot deposition or soot emission, and therefore an additional method is needed for this purpose.

Soot measurements in flames can be used to gain insights in the potential amount of soot available for deposition or emission. This avoids the use of exhaust gas emission measurements which can reflect the idiosyncrasies of individual appliances instead of the actual sooting tendencies of the fuel gases. In this paper a new method is presented which can predict a minimum soot volume fraction in flames, which is used to represent the soot available for deposition and emission in various types of appliances. The method is based on soot measurements performed using Laser Induced Incandescence in rich-premixed Bunsen-type flames with varying fuel compositions.

\* Corresponding author: Pieter.Visser@dnvgl.com  
International Gas Union Research Conference 2014

## 2. Procedure and experimental setup

### 2.1 Laser Induced Incandescence

Laser Induced Incandescence (LII) is based on heating soot particles up to the vaporization temperature of approximately 4000K by using a high energy laser pulse and the subsequent detection of the resulting emission. The conceptual simplicity of LII and the straightforward experimental setup of the technique make it popular for the determination of soot volume fractions in flames. In the present analysis, it is assumed that the absorbing soot particles in the early stage of soot formation are small enough to use the Rayleigh scattering criteria [3, 10]:

$$\pi d_p / \lambda < 0.3 \quad (1)$$

In equation (1)  $d_p$  is the average diameter of the soot particles and  $\lambda$  is the wavelength of the laser. It is this condition that results for the soot particles to absorb the incident laser light approximately in proportion to their volume. The selection of the incident laser light wavelength is thus an important factor for LII measurements. However, in LII the emitted incandescence at a certain detection wavelength ( $\lambda_{\text{det}}$ ) is measured. A theoretical study revealed that the peak of the LII signal in the Rayleigh regime is proportional to the average soot particle diameter as stated in equation (2) [3,4]:

$$\text{LII signal} \propto N_p d_p^x \quad (2)$$

Here  $N_p$  is the number of soot particles and  $x=(3+0.154/\lambda_{\text{det}})$  with  $\lambda_{\text{det}}$  being the detection wavelength. Equation (2) indicates that a linear relationship between the LII signal and the volume fraction can only be assumed for longer detection wavelength where  $x$  approaches 3.

Interferences from Laser Induced Fluorescence (LIF) from other combustion products should be considered when choosing the detection wavelength. In soot diagnostics, interferences mainly result from LIF of polycyclic aromatic hydrocarbon (PAH) species, which absorb and fluoresce in broad regions of the UV and visible spectrum. Fluorescence from PAH species can be induced by the second harmonic of an Nd-YAG laser at 532 nm, an often used wavelength for optical diagnostics. At the fundamental laser line of 1064 nm no fluorescence from PAH species will be induced; therefore for the measurements described in this paper this wavelength is used. The choice of excitation wavelengths to avoid potential interferences is a powerful feature of LII and one that is widely exploited in practice [3].

Figure 1 shows a schematic overview of the optical setup used for the LII measurements. A pulsed Nd:YAG laser (Quanta-Ray Pro-Series, Spectra-Physics) operating at 1064 nm is used with a frequency of 10 Hz and a pulse length of approximately 10 ns. A variable optical attenuator was used to adjust the power of the laser. Using a beam splitter a part of the laser beam is diverted to a power meter to determine the laser power. A lens ( $f=500\text{mm}$ ) is used to focus the laser beam in the flame. The incandescence signal was detected under a 90 degree angle by a quartz camera lens (Nikkor  $f/4.5$ , 300 mm) mounted on a gated intensified CCD camera (PI-MAX, Princeton Instruments, 25  $\mu\text{m}$  pixel size, 1024 x 256 pixels). A bandwidth filter centered at 400 nm (FWHM = 10 nm) was used to reduce the interference from laser-produced C2 and other carbon species [3]. The gating was coordinated by a generator (DG-535, Stanford Research) and monitored using a 100 MHz oscilloscope (Hewlett Packard 54600B). During all experiments the detector gate is triggered promptly with the arrival of the 1064-nm laser pulse at the measurement volume using a 100 ns gate width. The LII images were obtained with a series of 45 individual images each consisting of the accumulation of 10 shots. All LII signals were collected and saved with the Winspec/32 (Princeton Instruments) software.

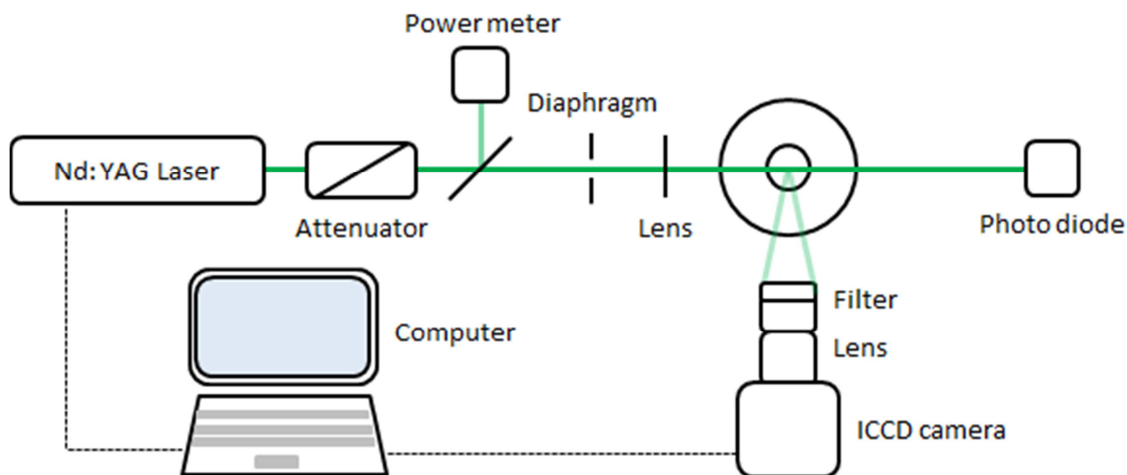


**Figure 1: Schematic overview of the LII setup.**

As LII measurements are performed by heating soot particles up to their vaporization temperature of approximately 4000K it is important to ensure the laser intensity is sufficient for this purpose. The laser intensity was increased to the point at which the ‘plateau’ region was just reached, above 48 mJ per pulse, the region in which the LII signal no longer increases with intensity [3, 5-8].

## 2.2 Coflow diffusion burner setup

In Figure 2 a schematic overview is shown of the coflow diffusion burner used in the experiments. The central pipe through the burner with a diameter of 7 mm is used to supply the fuel or the rich-premixed fuel/air mixture during the experiments. A coflow of air is used with a sufficient flow to stabilize the flame. In the coflow supply pipe glass beads were used to homogenize the velocity profile of the air. Above the burner a chimney was installed to further stabilize the flame.

A 3-D positioner (Parker Corp.) was used to position the burner and move the flame through the laser to perform measurements as function of distance from the burner. The flows of the individual gases in the gas/air mixture and the coflow were measured using calibrated mass flow meters (Bronkhorst, EL-FLOW). The overall reproducibility of the LII measurements was better than 10%.

In most gas-fired end-use appliances a change in fuel composition (density) results in a change in fuel flow rate. To simulate this behavior during the experiments a methane diffusion flame with a flow rate of 356 mL/min was used as a reference. The flow rate for every other measured gas composition was calculated using Bernoulli’s principle (which states that the flow rate through an orifice is inversely proportional to the density of the fuel). Next for the pure diffusion flames, the flame length, here defined as the distance between the burner and the secondary mantle of the flame, was measured for each new gas composition (e.g.  $\text{CH}_4/\text{C}_3\text{H}_8$ ). At a constant flame length air was added to the fuel and the soot volume fractions were measured for different equivalence ratios. The reason for keeping the flame length constant when adjusting the equivalence ratio was to maintain the stability of the rich-premixed flames. The restriction in flame lengths does not influence the end results of the soot model as will be discussed below.

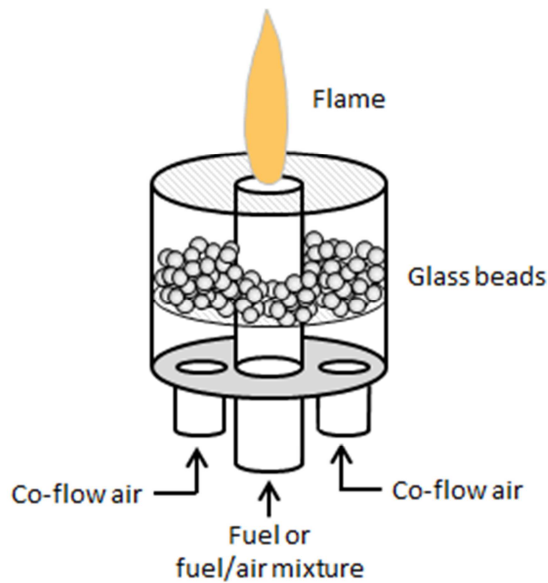


**Figure 2: Schematic representation of the coflow diffusion burner used in the experimental work.**

### 3. Experimental results

For quantitative measurement of the soot volume fraction with LII, the results of the measurements in this paper were compared to previous measurements [9], in which light extinction methods were used to calibrate the LII signal. The same burner and experimental conditions (pure diffusion flame using methane as a fuel, identical flow conditions) were used for a direct comparison of the previous soot volume fraction and the current LII signal in the same flame. The shape of the centerline soot volume fraction profile obtained here was identical to that found previously. All soot volume fractions in this paper have been quantified using this comparison.

#### 3.1 Measurements on 2-component mixtures

Here we describe the results of the LII measurements in 2-component gas mixtures; these include varying fractions of alkanes up to butane, hydrogen, nitrogen and carbon dioxide in methane. Figure 3 shows the results of the soot measurements in rich-premixed methane flames with approximately 5 mol% ethane, propane or n-butane. We note that the equivalence ratio at which soot formation is significant in the methane flame is at extremely fuel rich conditions: for example, an equivalence ratio of 15 corresponds to premixing approximately 7% of the required amount of air in comparison to stoichiometric conditions. Yellow tipping however can be observed with 25 – 50% of the required amount of air in comparison to stoichiometric conditions depending on the burner diameter and the gas composition [2]. The relatively large difference in the fraction of premixed air between yellow tipping and significant soot formation further emphasizes that a model developed for characterizing yellow tipping may not necessarily accurately predict soot formation or emission.

Figure 3 also shows that the soot volume fraction increases linearly with the equivalence ratio in this range of equivalence ratios, illustrated by the linear fit through the experimental data points. Although not shown in Figure 3, we note that at very high equivalence ratios the soot volume fraction no longer follows the linear fit line. For the pure methane diffusion flame a maximum soot volume fraction of approximately 400 ppb is reached. Also, at low equivalence ratios the soot volume fraction approaches zero. Therefore when the soot volume fractions would be measured across the entire range of equivalence ratio an S-curve would be obtained. For the development of the predictive soot model described below, measurements for all fuels were performed in the linear region.

From the results of the LII measurements for the  $\text{CH}_4/\text{C}_2\text{H}_6$ ,  $\text{CH}_4/\text{C}_3\text{H}_8$  en  $\text{CH}_4/\text{C}_4\text{H}_{10}$  gas mixtures it is found that, as expected, the addition of higher alkanes to methane increases the soot volume fraction at a constant equivalence ratio, see also Figure 3. Also the equivalence ratio at which a constant amount of soot is measured decreases with the addition of higher hydrocarbons to methane; soot formation occurs at ever increasing amounts of air premixing for higher fractions of higher hydrocarbons. Methane is observed to have a very low sooting tendency and even small fractions of higher hydrocarbons significantly increase the soot volume fraction in the flame at the same equivalence ratio. Although not shown in this figure, it is also important to note that the increasing the hydrocarbon (mole) fraction ( $\text{C}_2\text{H}_6$ ,  $\text{C}_3\text{H}_8$  or  $n\text{-C}_4\text{H}_{10}$ ) in methane increases the soot volume fraction.

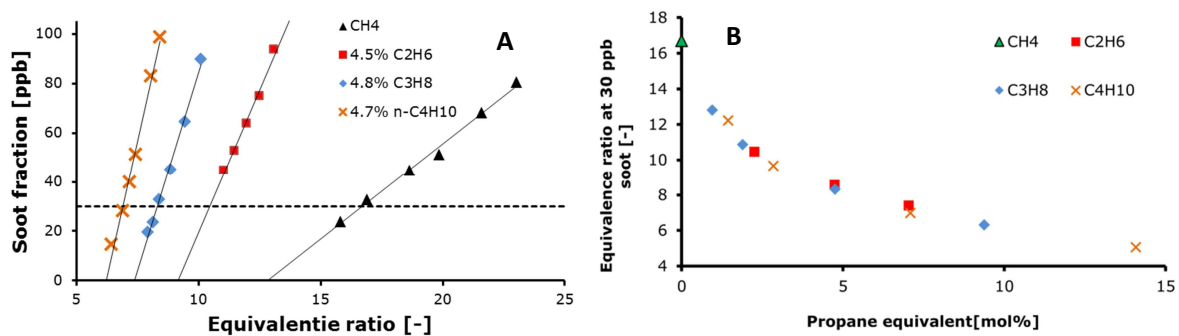


**Figure 3: A. Soot volume fractions in rich-premixed  $\text{CH}_4$ ,  $\text{CH}_4/\text{C}_2\text{H}_6$ ,  $\text{CH}_4/\text{C}_3\text{H}_8$  and  $\text{CH}_4/n\text{-C}_4\text{H}_{10}$  flames as a function of equivalence ratios. The dotted line denotes the arbitrarily chosen fixed soot amount (30 ppb, see text for details), B. Equivalence ratio for soot fraction of 30 ppb as a function of PE**

As can be seen in Figure 3B the equivalence ratio at which a fixed amount of soot is produced, in this case an arbitrarily chosen 30 ppb, is observed to scale with the propane equivalent (PE<sup>1</sup>) for binary mixtures of higher hydrocarbons. It should be noted that this relation is not valid for gas mixtures containing non-hydrocarbon species.

The equivalence ratio at which a constant amount of soot is measured increases after the addition of nitrogen, carbon dioxide and hydrogen to methane; the amount of air in the gas/air mixture needs to be decreased to obtain a significant amount of soot in the flame. Conversely, at the same equivalence ratio a lower soot volume fraction is measured with increasing amounts of these gases. It should be noted that the effect on the sooting tendency was found to increase from hydrogen to carbon dioxide for the same addition ( $\text{H}_2 < \text{N}_2 < \text{CO}_2$ ). Figure 4 illustrates the effects of hydrogen on soot formation in methane flames.

<sup>1</sup> The propane equivalent fraction is calculated as:  $\text{PE} = 0.5 \cdot \text{C}_2\text{H}_6 + 1 \cdot \text{C}_3\text{H}_8 + 1.5 \cdot \text{C}_4\text{H}_{10} + \dots$

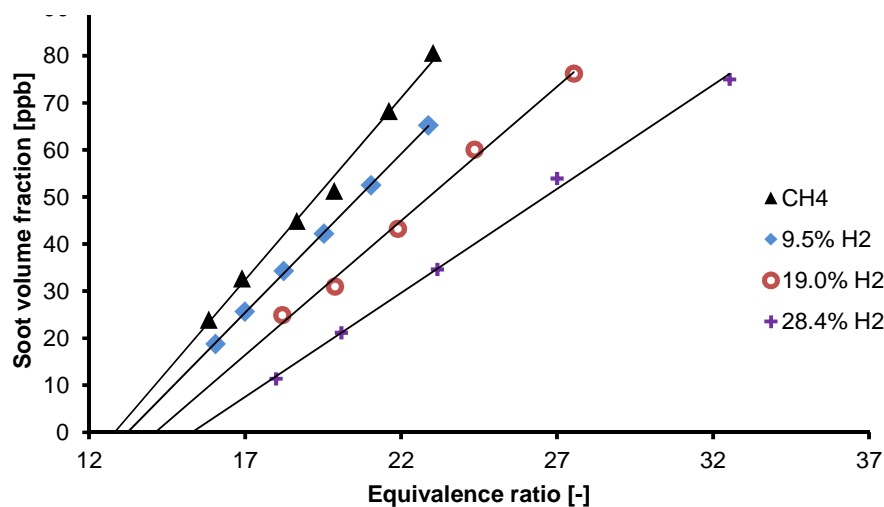


Figure 4: Soot volume fractions in rich-premixed CH<sub>4</sub>/H<sub>2</sub> flames as a function of equivalence ratios.

### 3.2 Measurements on 3- and 4-component mixtures

Measurements were further performed on 3- and 4-component mixtures. To study the effect of hydrogen and inert gas addition on the sooting tendencies in ternary mixtures, a couple of measurements were performed on CH<sub>4</sub>/C<sub>3</sub>H<sub>8</sub>/N<sub>2</sub>, CH<sub>4</sub>/C<sub>3</sub>H<sub>8</sub>/CO<sub>2</sub> and CH<sub>4</sub>/C<sub>3</sub>H<sub>8</sub>/H<sub>2</sub> fueled flames with a fixed amount of propane, approximately 9.3%. These results were compared to the binary CH<sub>4</sub>/C<sub>3</sub>H<sub>8</sub> mixture with a similar amount of propane. Similar to the behavior observed upon addition of these gases to methane, the addition of carbon dioxide and nitrogen to a CH<sub>4</sub>/C<sub>3</sub>H<sub>8</sub> mixture has a decreasing effect on the soot volume fraction at a constant equivalence ratio. For hydrogen however, deviant behavior is observed. As shown in Figure 5, the addition of 5.3% hydrogen to the CH<sub>4</sub>/C<sub>3</sub>H<sub>8</sub> mixture seems to decrease the soot volume fraction, but the soot volume fraction seems to remain constant or even *increase* within the uncertainty of the method upon addition of 10.9% and 20.8% hydrogen at a constant equivalence ratio. This behavior for hydrogen is at present poorly understood.

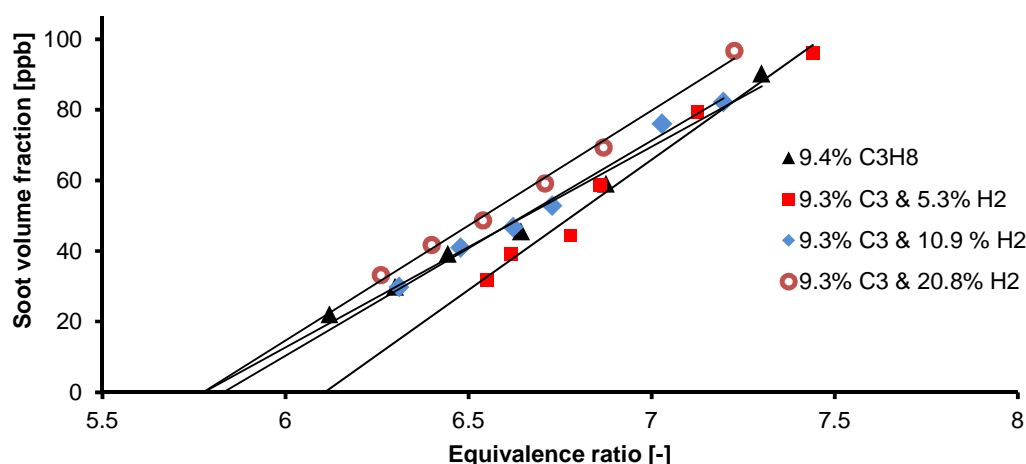


Figure 5: Soot volume fractions in rich-premixed CH<sub>4</sub>/C<sub>3</sub>H<sub>8</sub>/H<sub>2</sub> flames as a function of equivalence ratios.

In addition to the results presented above, nine more 3- and 4-component mixtures were measured. We also note that, apart from the effect of hydrogen on soot formation described above, the effect of different fuel components on the soot volume fraction is qualitatively in agreement with the behavior

observed in pure diffusion flames. We therefore expect that the trends observed in soot volume fraction with varying fuel composition will still be valid outside of the linear region, i.e., at equivalence ratios higher than those presented in this paper.

#### 4. Model development

We here describe a model with which gas compositions can be compared in terms of their sooting tendencies based on the experimental results. Whilst a prediction of the soot fraction per gas composition would be useful, this is currently too complex to model. Instead therefore we develop a model that can predict the equivalence ratio yielding a given, constant, soot fraction. This model enables us to characterize gases for their soot tendency.

In total 40 binary, 3- and 4-component mixtures are used as input for the model. For each of these mixtures and methane the relationship between soot volume fraction and equivalence ratio were fitted in the linear region of the graphs. Based on the fit we calculated the equivalence ratio at which we (arbitrarily) expect a soot volume fraction of 30 ppb; this “critical” equivalence ratio is denoted as  $\phi_{30 \text{ ppb}}$ . It should be noted that a different critical equivalence ratio (i.e., using a different soot volume fraction) could be chosen with similar results. The values for  $\phi_{30 \text{ ppb}}$  were used in a regression analysis to be able to predict  $\phi_{30 \text{ ppb}}$  based on the gas composition. In the regression analysis most of the individual fractions of the different components were used as variables, including quadratic terms. For the higher alkanes the PE serves as an additional variable due to the excellent fit between  $\phi_{30 \text{ ppb}}$  and PE, as can be seen in Figure 3B. This correlation reduced the number of variables significantly. After an optimization of the model a total of 9 variables remained. The fit through the data points was significantly improved by this optimization and the ability of the model to predict  $\phi_{30 \text{ ppb}}$  was modest only in the region with practically no soot (for example in gas compositions with high fractions of inert gases without any higher hydrocarbons). Table 1 shows the 9 remaining variables and their coefficients to predict a value for  $\phi_{30 \text{ ppb}}$  according to equation (3):

$$\phi_{30 \text{ ppb}} = \sum_{i=0}^9 B_i \cdot X_i \quad (3)$$

**Table 1: Variables in the regression equation to predict  $\phi_{30 \text{ ppb}}$  \*.**

Coefficient	$B_i$	$X_i$
0	75.523	1
1	-58.964	$(X_{\text{CH}_4})^2$
2	-3.950	PE
3	$3.088 \cdot 10^{-1}$	$(\text{PE})^2$
4	$-9.938 \cdot 10^{-3}$	$(\text{PE})^3$
5	-61.422	$X_{\text{C}_2\text{H}_6}$
6	-34.969	$X_{\text{C}_3\text{H}_8}$
7	-81.190	$X_{\text{n}_2}$
8	-73.913	$X_{\text{CO}_2}$
9	-94.992	$X_{\text{H}_2}$

\*The regression analysis is valid for the following fractions:

$\text{CH}_4$  0.7 – 1.0,  $\text{C}_2\text{H}_6$  0 – 0.145,  $\text{C}_3\text{H}_8$  0 – 0.095,  $\text{C}_4\text{H}_{10}$  0 – 0.095,  $\text{N}_2$  0 – 0.2,  $\text{CO}_2$  0 – 0.2,  $\text{H}_2$  0 – 0.2  
 PE 0 – 15;  $5 \leq \phi_{30 \text{ ppb}} \leq 20$

The regression equation has been used to calculate  $\phi_{30 \text{ ppb}}$  from measured gas compositions. The predicted values are plotted against the measured values in Figure 6. The data points are fitted using a least-squares fit. From the regression analysis a standard deviation of  $\phi_{30 \text{ ppb}}$  of 0.85 is found.

It should be noted that a small deviation in the value for  $\phi_{30 \text{ ppb}}$  can have a large impact on the soot fraction in flames; this effect is particularly large for rich gas mixtures. The difference in  $\phi_{30 \text{ ppb}}$  between a gas mixture of 9.5% ethane with  $\phi_{30 \text{ ppb}}= 8.6$  and 14.1% ethane with  $\phi_{30 \text{ ppb}}=7.4$  for example is only 1.2. This difference in the critical equivalence ratio is numerically small but the soot volume fraction increases from 30 ppb for 9.5% ethane to 83 ppb for 14.1% ethane, a difference of almost a factor of 3. This example illustrates a method to use the data and the model developed from it as an interchangeability tool for pipeline gases.

We note that the validity of the developed model is limited to the region in which  $\phi_{30 \text{ ppb}}$  is between 5 and 20, which corresponds to the values shown in Figure 6.

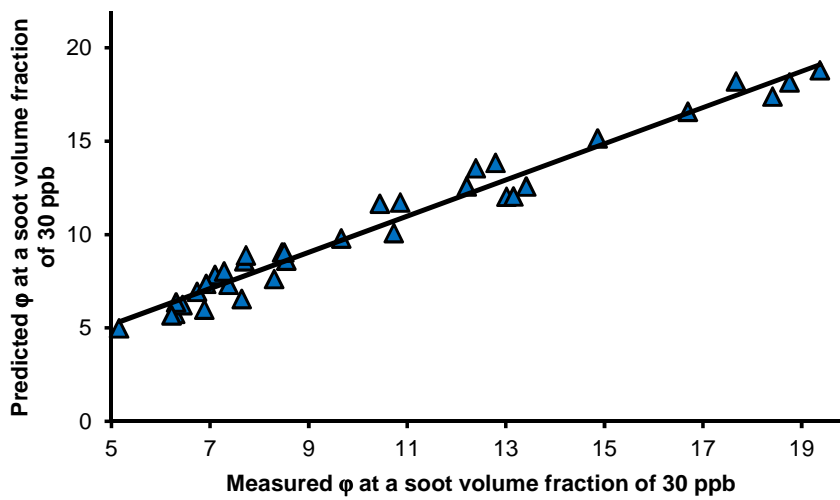


**Figure 6: Prediction of  $\phi_{30 \text{ ppb}}$  plotted against the measured value of  $\phi_{30 \text{ ppb}}$  from left to right the tendency for soot formation of the gas mixtures decreases.**

The ranking of gas mixtures on their soot tendencies is possible using the model developed because the fit lines in which the soot volume fractions are plotted against the equivalence ratio do not cross. This means that, in the linear region, choosing a different soot volume fraction for defining the critical equivalence ratio will yield the same ranking of gases in terms of sooting tendency.

The value for  $\phi_{30 \text{ ppb}}$  can be seen as a critical equivalence ratio at which soot begins to form at a given gas composition. As mentioned before a soot volume fraction other than 30 ppb could be chosen without influencing the ranking of gases in terms of sooting tendencies. Analogous to the approach in [3] where a critical equivalence ratio was chosen based on yellow tipping, the value for  $\phi_{30 \text{ ppb}}$  of a given gas composition can be compared to  $\phi_{30 \text{ ppb}}$  of a reference gas to compose an index for soot formation. With this index one can indicate whether the soot formation, soot emission or soot deposition is expected to increase or decrease. Here we remark that for appliances without fuel-to-air control variation gas compositions results in a change in the equivalence ratio.

To illustrate how the methodology can be used to characterize the soot tendencies of gases in appliances we use the following example; an appliance is fueled with gas 1 (Table 2) and operates at an equivalence ratio identical to the critical sooting equivalence ratio of  $\phi_{30 \text{ ppb}}=12.3$  (Table 2). When the equivalence ratio of the fuel/air mixture fed to the appliance is smaller than the critical soot equivalence ratio, the soot emission is below the critical value. Changing the gas composition from gas 1 to gas 2 (Table 2) results in a change in the critical soot equivalence ratio from  $\phi_{\text{critical}}=12.3$  to 9.6. Thus for appliances with a fuel-to-air control changing the gas composition from gas 1 to gas 2 results in an increase in sooting tendency ( $\phi_{30 \text{ ppb}} \leq \phi_{\text{appliance}}$ ). For appliances without fuel-to-air control the changes in soot tendency are



caused not only by the changes the critical soot equivalence ratio  $\phi_{30 \text{ ppb}}$  of the fuel but also due to the changes in the equivalence of the appliance itself. For these appliances the equivalence ratio of the appliance shifts from  $\phi=12.3$  to 12.8 which means that the soot fraction will be higher than for appliances with fuel-to-air control (Table 2).

**Table 2: Comparison of sooting tendencies of two gases**

Fractions	1	2
CH <sub>4</sub>	0.797	0.800
C <sub>2</sub> H <sub>6</sub>	0.029	
C <sub>3</sub> H <sub>8</sub>	0.020	0.060
C <sub>4</sub> H <sub>10</sub>	0.002	
N <sub>2</sub>	0.143	0.140
CO <sub>2</sub>	0.009	
PE	3.750	6.000
$\phi_{30 \text{ ppb}}$	12.3	9.6
Wobbe Index (MJ/m <sup>3</sup> (n))	44.4	46.2
$\phi$ appliance (with fuel-to-air control)		12.3
$\phi$ appliance (without fuel-to-air control)		12.8

## 5. Summary and Conclusions

The results of Laser-Induced Incandescence measurements in rich-premixed Bunsen-type flames fueled with methane, higher hydrocarbons up to butane, nitrogen, carbon dioxide and hydrogen were presented. The experiments show that the soot volume fractions measured in methane diffusion flames is relatively small. The addition of even small fractions of ethane, propane and butane increases the soot volume fraction significantly. Butane has the strongest increasing effect and ethane the weakest. A correlation was observed between a propane equivalent composition of higher alkanes and the actual soot volume fractions for the hydrocarbons examined. The addition of nitrogen, carbon dioxide and hydrogen decrease the soot volume fractions, here the strongest decreasing effect is observed in carbon dioxide and the weakest in hydrogen.

Soot fractions were also measured in tertiary mixtures with approximately 9.3% propane and increasing amounts of nitrogen, carbon dioxide and hydrogen. For nitrogen and carbon dioxide the same qualitative behavior was observed as before in methane, i.e. the soot volume fractions decreased upon the addition of these inert gases in the tertiary mixtures. For hydrogen however, the addition of 5.3% hydrogen to the CH<sub>4</sub>/C<sub>3</sub>H<sub>8</sub> mixture seems to decrease the soot volume fraction, but the soot volume fraction seems to remain constant or even *increase* within the uncertainty of the method upon addition of 10.9% and 20.8% hydrogen at a constant equivalence ratio. This behavior for hydrogen is at present poorly understood.

In addition to the flames mentioned above LII measurements were performed on multiple 3- and 4-component fuel mixtures. Based on all measurements an arbitrarily chosen critical equivalence ratio of the fuel/air mixture was determined at which a minimum amount of soot was measured for all flames, in this case 30 ppb. The results obtained were used in a regression analysis which yielded an equation to predict the equivalence ratio where 30 ppb soot was measured as a function of variables related to the gas composition. When predicted values were plotted versus the measured values of the critical equivalence ratio the regression equation shows good predictive ability. The standard deviation is sufficiently small to rank different gases on their actual soot tendency with a reasonable accuracy. The

equation can be used to analyze the soot tendency at varying gas compositions at equivalence ratios where soot formation, deposition and emission may occur.

## Acknowledgement

The authors would like to acknowledge the assistance of A.V. Mokhov from the Laboratory for High Temperature Energy Conversion Processes at the University of Groningen in performing the Laser-Induced Incandescence experiments.

This research has been financed by a grant from the Energy Delta Gas Research (EDGaR) program. EDGaR is co-financed by the Northern Netherlands Provinces, the European Fund for Regional Development, the Ministry of Economic Affairs, Agriculture and Innovation and the Province of Groningen. We also gratefully acknowledge the financial support from the N.V. Nederlandse Gasunie.

## References

- [1] Levinsky, H.B., *“Report of Identification of the concentration and combination of higher hydrocarbons in natural gas likely to cause sooting in gas appliances”*, Doc. Nr. URN 05/1943 Department of Trade and Industry UK (2005)
- [2] Grumer, J., Harris, M.E. and Rowe, V.R., *“Report of Investigations 5225”*, US Bureau of Mines, Pittsburgh, PA (1956)
- [3] Kohse-Hoinghaus, K. and Jeffries, J.B., *“Applied Combustion Diagnostics”* Taylor & Francis, New York (2002)
- [4] Melton, L.A., *“Soot Diagnostics Based on Laser Heating”*, Appl. Optics, vol. 23, pp. 2201–2208 (1984)
- [5] Ni, T., Pinson, J.A., Gupta, S. and Santoro, R.J., *“Two-Dimensional Imaging of Soot Volume Fraction by the Use of Laser-Induced Incandescence”*, Appl. Optics, vol. 34, pp. 7083–7091 (1995)
- [6] Shaddix, C.R. and Smyth, K.C., *“Laser-Induced Incandescence Measurements of Soot Production in Steady and Flickering Methane, Propane, and Ethylene Diffusion Flames”*, Combust. Flame, vol. 107, pp. 418–452 (1996)
- [7] Vander Wal, R.L. and Jensen, K.A., *“Laser-Induced Incandescence: Excitation Intensity”*, Appl. Optics, vol. 37, pp. 1607–1616 (1998)
- [8] Witze, P.O., Hochgreb, S., Kayes, D., Michelsen, H.A., and Shaddix, C.R., *“Time-Resolved Laser-Induced Incandescence and Laser Elastic-Scattering Measurements in a Propane Diffusion Flame”*, Appl. Optics, vol. 40, pp. 2443–2452 (2001)
- [9] Buitrago, J.E., Mokhov, A.V., Levinsky H.B. and Smooke, M.D., *“Experimental and Computational Study of Soot Formation in Laminar, Axisymmetric Methane/Hydrogen Diffusion Flames”*, 20<sup>th</sup> Journee d’Etudes of the Belgian Section of the Combustion Institute, May 2008, Ghent.
- [10] Schulz, C., Kock, B.F., Hofmann, M., Michelsen, H., Will, S., Bougie, B., Suntz, R. and Smallwood, G., *“Laser-induced incandescence: recent trends and current questions”*, Appl. Phys. B 83(3), pp. 333-354 (2006)